45th AIAA Aerospace Sciences Meeting and Exhibit
8 - 11 January 2007, Reno, Nevada
AIAA-2007-0390
AIAA-2007-0390

Interaction of a Gaseous Fuel Jet with Shock-Wave-Rich Airflow

A. Abdelhafez* **and A. K. Gupta†**
Department of Mechanical Engineering, University of Maryland, College Park
College Park, MD 20742

K. H. Yu‡
Department of Aerospace Engineering, University of Maryland, College Park
College Park, MD 20742

The mixing of a gaseous fuel jet injected into a shock-wave-rich supersonic airflow has been examined. Different airflow Mach numbers and injection configurations (parallel, oblique, and normal) have been investigated numerically using a validated code. It was found that the shock-wave-rich environment, i.e. the shock train of the airflow, aids to a great extent in mixing enhancement for all injection configurations, especially at small oblique injection angles close to the parallel configuration. Unlike what was shown in previous research on fuel injection in shock-free supersonic airflows that normal or oblique injection at angles as large as 30° or 60° is inevitable to achieve sufficient mixing, substantial mixing improvement is provided by shock-wave-rich airflows. Fuel injection at small oblique angles of only about 5° improves mixing while minimizing the pressure losses accompanying the fuel injection, which leads to increased thrust. Due to the lack of experimental data for validation, the code was validated by using it to numerically simulate part of the results of a past experimental investigation from the literature. Good agreement of the simulation results and the actual flowfield data was observed. The global features of the flow under high-speed conditions are similar to those reported previously, so that our results of mixing in shock-rich supersonic flows provide good insights on a more favorable fuel injection configuration that provides better mixing with lower losses and higher thrust.

I. Introduction

ALTHOUGH many of the future high-speed vehicles will be powered by scramjet engines, mixing and ignition in such engines have not yet been fully understood in detail. Improving the performance of such engines is directly affected by the quality of fuel-air mixing, which consequently affects the ignition and combustion. In many instances, the equivalence ratio of operation has to be fuel-rich to ensure the presence of a flame that provides positive thrust. Therefore, any progress made on improving the engine efficiency must be closely followed towards achieving efficient mixing between the fuel and air. At the high speeds of scramjet flows, where the residence time is of the order of a millisecond, efficient mixing becomes critical, as it directly relates to the length of the combustor, which, in turn, affects the vehicle weight, available payload, developed thrust, and specific impulse.

Previous research has shown that flame holding in supersonic reacting flows is achieved by the creation of a re-circulation zone, where the fuel and air are partially mixed at low velocities[1]. In the case of transverse (normal) injection of fuel from a wall orifice, see Figure 1a, a bow shock is produced as a result of the direct interaction of the fuel jet with the supersonic cross-flow. Consequently, the upstream wall boundary layer separates, providing a region where the boundary layer and the fuel jet mix subsonically upstream of the jet exit. This region was reported to be important in the transverse-injection flowfield because of its flame-holding capability in the reacting situations. Several studies have been conducted on this issue[2,3]. Autoignition was observed at the upstream recirculation region of the jet and behind the bow shock. However, this injection configuration has stagnation pressure losses due to the strong three-dimensional bow shock[4] formed by the normal jet penetration, particularly at high flow velocities. On the other hand, it is possible to reduce those pressure losses by performing angled (oblique) injection, so that the resulting bow shock is weaker, see Figure 1b. In this approach, the axial momentum of the fuel jet can also contribute to the net engine thrust. However, ignition occurs only far downstream of the jet in this case.

These observations are true, but only for shock-free supersonic flows, i.e. flows that do not contain any shock waves of their own in the absence of fuel injection. In an

* Graduate Student, Student Member AIAA
† Professor, Fellow AIAA, Email: akgupta@eng.umd.edu
‡ Associate Professor, Associate Fellow AIAA

experimental investigation[5], a supersonic hydrogen flame (with coaxial hydrogen injection) was stabilized along the axis of a Mach 2.5 wind tunnel. Flame stabilization was achieved using wedges mounted on the tunnel sidewalls to generate oblique shock waves that interact with the flame. It was found that the shock waves enhance the fuel-air mixing to the extents that the flame lengths decreased by up to 30%, when certain shock locations and strengths were chosen that are optimum for the investigated geometry and flows. The researchers explained that the conditions of optimum shock locations and strengths prevail when the primary shocks are positioned to interact with the flame base and the downstream recompression shocks, determined by the wedge location and size, interact with the central portion of the flame. Their experimental results have shown that, for the investigated flows and geometry, best mixing and stability correspond to 10° wedges placed at an upstream position four times the fuel jet diameter. The researchers reasoned that enhanced mixing resulted, in part, because the shocks turn the flow and induce radial inflows of air into the fuel jet. The reason for the significant improvement in flame stability is believed to be due to the adverse pressure gradient caused by the shock, which can elongate the recirculation zone. It was concluded that optimization of the mixing and stability limits requires a careful matching of the shock strength and the location of shock/flame interaction.

In another investigation[6], shock-induced mixing was simulated numerically, where parallel flows of a heavy gas interspersed with other flows of a lighter one were overtaken by a normal shock wave. It was shown that the interaction of the density gradient at each light/heavy interface with the pressure gradient imposed by the shock wave generates vorticity that causes the light gas regions to roll up into one or more counter-rotating vortex pairs, which stir and mix the light and heavy gases together. These two-dimensional flows are analogous to three-dimensional flows that may be found in scramjet combustors, demanding rapid and efficient mixing of fuel and oxidizer. It was concluded that, whenever possible, multiple shock waves should be utilized.

Oblique shock waves that form within a scramjet combustor are often unavoidable (Figure 2), yet they may have positive effects on fuel-air mixing and flame stabilization, even in the cases of parallel or small-angle oblique injection[7]. In general, shock waves can affect a flame because they can (a) direct the airflow traversely (towards the fuel) and thus increase the entrainment rate, (b) create additional vorticity which enhances the mixing rates, (c) create an adverse pressure gradient which elongates the flame recirculation zones, and (d) increase the static pressure and temperature. The exact role of each effect needs further substantiation and quantification. The objective of the present work is to numerically simulate the effects of shock waves on the flowfield and mixing in shock-rich supersonic flow, over a range of fuel injection angles. The goal is to enhance mixing while reducing the injection pressure losses.

II. Simulation Matrix and Assumptions

In order to simulate the positive effects of a shock-wave-rich environment on mixing, a circular convergent-divergent nozzle was selected (Figure 3a). The divergent (supersonic) part of this nozzle contains four equally-spaced ramps of 1° each, so as to generate a shock train. This nozzle design aims only at examining mixing enhancement in a shock-wave-rich environment and not at closely simulating actual scramjet flows, since the shock train generated by this nozzle was found to be strong enough to decelerate the flow from supersonic Mach numbers in the first half of the divergent section to subsonic speeds in the second half. Under the assumption of axisymmetric, two-dimensional flow, only half of the nozzle geometry has been simulated to reduce the computation time. A concentric fuel system was selected (Figure 3b) to facilitate injection in different configurations from parallel to oblique and normal (traverse), which has many practical implications for direct relevance on the utilization of the results obtained. A 0.18-in (4.6-mm) injection port was selected for parallel injection, whereas the oblique/normal injection system comprises six 0.073-in (1.9-mm) injection ports, the total area of which is equal to that of the single parallel injection port. A recess length of 5 mm was chosen, as shown in Figure 3b, in order to ensure that (a) the fuel is injected into a supersonic airflow, and (b) the fuel core has an axial distance of about 40 – 50 mm downstream of the location of injection while still being surrounded by the shock-wave-rich supersonic airflow, before the air eventually decelerates to subsonic speeds close to the nozzle exit.

The ESI-Group CFD-FASTRAN 2007 LES-based code was used for all the simulations reported in this study. Due to the lack of experimental validation, part of the experimental work done by Huh and Driscoll [5] was simulated here, to provide some code validation. Thus, the necessary validation is provided here in form of a comparison of the simulation results to the actual flowfield data obtained by Huh and Driscoll. This comparison is depicted in Figure 4. It can be seen from the Schlieren density gradients (which give a very good visualization of the flow shock train and pressure gradients) that the actual flowfield data are in good agreement with the simulation results, especially the contours of static pressure and Mach number, which demonstrates the capability of the CFD-FASTRAN code of capturing the fine features of the flowfield and providing credible simulation results.

Throughout the different simulations conducted in this work, the Spalart-Allmaras turbulence model was implemented with constant eddy viscosity for both the air and fuel inlets. The viscosity and conductivity were computed based on the kinetic theory of gases, while the mass diffusivity was computed based on Fick's law with a Schmidt number of 0.5. A turbulent Prandtl number of 0.9 was used for the calculation of the turbulent conductivity. The air inlet was

assigned the boundary condition type "fixed total pressure and temperature", so that these two quantities of the air inlet would be preserved throughout the iteration process until the convergence criteria are met. A total temperature of 300 K was selected for the air inlet in all the cases presented in this work, whereas the total pressure was assigned the value corresponding to the desired case Mach number from the one-dimensional isentropic flow relations. Preserving the total pressure and temperature throughout the iteration process ensures that the desired case Mach number will be achieved. Fuel was simulated by helium, as these simulated results provide a basis for their experimental validation to be obtained in our laboratory in the near future. Unlike air, which has a speed of sound of only 330 m/s at atmospheric temperature, both hydrogen and helium have sound velocities as high as 1300 and 1000 m/s, respectively. Thus, although fuel-rich conditions were chosen for most examined cases in this work, which led to helium velocities as high as 300 m/s, the helium flow was still considered incompressible (helium Mach number ≤ 0.3). Consequently, the flow of helium through the fuel injection system prior to injection was not simulated; instead the conditions at the injection port were fed directly into the simulation space to reduce the size of the computational grid and, therefore, the computation time. The boundary condition type "fixed flow rate" was assigned to the fuel inlet, because the amount of injected fuel is controlled using mass flow controllers in our experimental efforts. For all cases presented in this work, the pressures of helium at the injection port were selected to be as close as possible to the throat pressure of the airflow in the absence of fuel injection, so as to minimize the total pressure losses of the airflow due to fuel injection at a pressure different from the local static pressure of air upstream of the fuel injection port.

The properties at the nozzle exit plane, particularly the pressure, were not fixed throughout the iteration process of each simulated case. Instead, the exit plane was set to be "extrapolated." Thus, for each time step of the iteration process, the code iterates internally on the spatial dimensions (i.e., axially and radially) in a marching manner from the fixed conditions at the nozzle inlet towards its exit, and updates the properties of the exit plane accordingly. The nozzle walls were set to be isothermal at 300 K, because the actual nozzle (to be tested experimentally in the near future) has thick aluminum walls that will behave as an almost-perfect heat sink, as estimated from preliminary heat transfer calculations. The walls of the fuel system, on the other hand, were set to be adiabatic, because, first, the actual fuel system will be made of stainless steel that has a much lower thermal conductivity (relative to aluminum), and second, the fuel system is immersed almost totally into the air delivery system and nozzle, which allows for negligible amounts of heat to be conducted axially upstream through the thin walls of the fuel system.

The initial conditions of simulation were set equal to those of the air inlet for each simulated case, i.e. velocity, static temperature, and eddy viscosity, except for the static pressure, which was set to its atmospheric value, so as to simulate the flow behavior once the air supply valve is opened in an experimental test facility, thus allowing the high-pressure air to expand and "march" through the nozzle from inlet to exit. A total of 2500 iterations or cycles were made for each simulated case; convergence was usually attained after 2300 – 2400 iterations. Table 1 lists the simulated matrix presented here. The investigated cases are divided among two analyses; the first examines the effect of changing the polar angle of injection from zero (parallel) to 5°, 10°, and 30° (oblique), to 90° (normal), keeping the nominal maximum air Mach number fixed at 2.7 and the fuel Mach number at 0.25. The nominal maximum air Mach number is defined here as the maximum local Mach number of the airflow attainable in the absence of fuel injection, i.e. at no total pressure losses due to fuel injection. The second analysis examines the effect of changing the nominal maximum airflow Mach number from 2.4 to 2.7 and 3.0 for a fixed polar angle of injection of 5° (oblique) while keeping the fuel flow rate constant at its value from the previous analysis (called analysis I), in order to facilitate a comparison based on the fuel mass fraction profiles. Note that cases I-b and II-b are the same case (see table 1).

III. Results and Discussion

Effect of Injection Scheme

The Mach number, static pressure, and helium mass fraction profiles for cases I-a to I-e are shown in Figures 5a to 5e, respectively. As observed from the Mach number profiles, supported by the static pressure, the flow undergoes a shock train, i.e., a series of shock waves, the existence of which is evidenced by the local steep gradients of Mach number and static pressure. Case I-a shows an extreme example, wherein the shock train affects the mixedness of helium without being much affected by the injected helium jet, because the latter is injected parallel to the airflow. Not being able to easily penetrate the resistive supersonic airflow, the expanding subsonic helium core, however, induces some minor shocks of weak strengths into the airflow, with the first shock originating at the edge of the helium inlet, where air first comes into contact with the helium jet. It can be clearly seen that, although the parallel air and helium flows are separated by a distinct supersonic-to-subsonic boundary or shear layer during the first 30 mm downstream of the injection port, the mixedness of helium improves substantially in the following 20 mm, i.e., between the axial locations of 0.04 and 0.06 m. This is attributed to the phenomenon of shock/shear layer interaction. The adverse pressure gradient across a shock wave impinging on the shear layer directs the airflow traversely towards helium, and vice versa, thus increasing the local mixedness. This adverse pressure gradient also creates additional vorticity that enhan-

Table 1. Simulation Matrix

Case	Nominal maximum air Mach number	Polar angle of injection	Configuration
ANALYSIS I			
I-a	2.7	0°	Parallel
I-b	2.7	5°	Oblique
I-c	2.7	10°	
I-d	2.7	30°	
I-e	2.7	90°	Normal
ANALYSIS II			
II-a	2.4	5°	Oblique
II-b	2.7	5°	
II-c	3.0	5°	

ces the mixing rates, as well. The impingement of shock waves on the shear layer might not be distinctly observable from the Mach number and static pressure contours shown in Figure 5. This, however, does not mean that the interaction does not exist, since the shock waves seen emanating from the ramps of the nozzle divergent section cannot just vanish into the airflow, unless they impinge on the air/helium shear layer. This impingement was proven in previous research to cause significant spreading of the shear layer downstream of the shock/shear layer interaction region[8], which increases the mixing efficiency. This becomes obvious from the helium mass fraction profiles shown here in Figure 5. The sharp drop in helium concentration along the centerline between the axial locations of 0.02 and 0.04 m can be attributed to roll-up vortices building up due to the induced vorticity at the shock/shear layer interaction region, which leads eventually to shear layer spreading and enhanced mixing.

Figure 5b shows the results of case I-b, where fuel is injected obliquely at an angle of 5°. Unlike the previous case, oblique fuel injection affects the shock structure of the airflow significantly by inducing new shock waves, most of which are reflections and interactions of the first one located just upstream of the injection port, because helium is now injected at a non-zero polar angle to the airflow. Since these new shocks are weak, the airflow accelerates to a maximum Mach number almost equal to that found in parallel injection, and the early stage of the nozzle divergent section becomes air-dominated, with the fuel flow confined only to the thin subsonic boundary layer adjacent to the walls of the injection system, downstream of the injection port. Both confinement and the richer shock wave environment of this case result in highly enhanced mixing, as evidenced by the reduction of the high helium concentration as early as the tip of the fuel injection system. The vortex-shaped regions of medium-to-low helium mass fraction (< 0.2) found downstream of the injection system can be attributed to the build-up of roll-up vortices, as a result of the induced vorticity at the shock/shear layer interaction region. Thus, the shear layer spreads, resulting in greater entrainment of the two streams.

As the polar angle of oblique injection is increased to 10° (case I-c) and 30° (case I-d), the shock wave at the injection port becomes stronger. Consequently, the air Mach number after this shock decreases, and the airflow suffers higher total pressure losses, which can be observed by comparing the values of the maximum local Mach numbers for the two cases and for the 5° case. As the polar angle of injection increases, and the local air Mach numbers decrease (on the average), the shock train of the divergent nozzle section gradually loses strength and, consequently, the role it plays in mixing enhancement. The boundary layer confining the injected helium grows in thickness (so-called blockage problem), because (a) the suppressing supersonic airflow is losing energy (lower total pressure), and (b) the helium jet itself is being injected in a direction further away from the wall. However, it can still be said that the trends observed for the 5° case prevail for the 10° and 30° cases, even if the quality of mixing degrades, as the injection angle increases, see Figures 5b to d. The induced vorticity due to the shock/shear layer interaction decreases but still plays its role in generating the roll-up vortices that spread the shear layer and allow for radial entrainment of the two streams.

For the transverse-injection case I-e (depicted in Figure 5e), the shock wave at the injection port becomes strongest in strength. Thus, this case has the weakest Mach number profile among all cases examined in analysis I. Mixing enhancement due to shock/shear layer interaction becomes minimal in this case, as evidenced from the fact that it takes as much as 65% of the length of the divergent nozzle section to achieve near-complete mixing. Figure 6 summarizes the results of analysis I by plotting both the maximum local Mach number and the mixing length against the polar angle of injection for the five cases examined in analysis I. While this length, though roughly estimated, gives a good approximation of the degree of mixing enhancement provided by the shock/shear layer interaction, the maximum local Mach number gives an indication of the total pressure loss of the airflow. Two important observations can be made from Figure 6. The first observation is that the Mach number drops immediately, as the injection is deviated from the parallel configuration. This is expected due to the introduction of new shock waves within the flow. The Mach number, however, remains almost constant for a range of small acute injection angles before it starts dropping asymptotically to its minimal value at normal injection, giving rise to a narrow range, in which the injection angle can be changed slightly to adapt for any changes in operating conditions without much affecting the total pressure of the flow. This range is approximately from 5° to 10° for the geometry investigated in this work. It should be noted, however, that this range depends on both the geometry investigated and the nominal maximum Mach number of

airflow. Different geometries or Mach numbers may have slightly different ranges. Nevertheless, the distinct conclusion can still be made that *small* angles of oblique injection are effective for shock-wave-rich flows. This conclusion is strengthened by the second observation to be made from Figure 6; near-complete mixing is achievable within smaller axial distances, if the injection angle is kept small. The case of 5° oblique injection shows superior performance here, and is, therefore, selected for further investigation in analysis II of this work. Furthermore, keeping the injection angle small has an additional advantage (not shown in Figure 6), which is the reduction of flow blockage in scramjet combustors. It is well known, and Figure 2 depicts this, that supersonic duct flows suffer significant blockage due to boundary layer growth. Injecting the fuel traversely creates a bow shock, the strength of which is usually sufficient to increase blockage and reduce the momentum of the boundary layer downstream of the injection point to the extent that boundary layer separation becomes inevitable at the locations of shock/boundary layer interaction. In addition to the undesired losses accompanying the separation of the boundary layer, spot wall heating occurs at the points of separation, which means an advanced cooling system is necessary. Knowing that the locations of these separation points are unstable and unpredictable, adds to the complexity of the problem. Thus, to minimize the problems of flow blockage and boundary layer separation, injection at small oblique angles is desirable.

Effect of Air Mach Number

Since the Mach number of airflow affects its shock structure for a given geometry, the effect of changing the nominal maximum air Mach number was investigated and is termed as analysis II in this work. This analysis was carried out by keeping both the injection angle and fuel flow rate fixed at their corresponding values of case I-b. The reason behind the choice of a constant flow rate was to facilitate a comparison based on the fuel mass fraction profiles. Note again that cases I-b and II-b are the same case.

The results presented in Figures 7a and 7b, which depict the Mach number and static pressure profiles, respectively, for cases II-a, b, and c, show that as the Mach number of airflow is increased, the shock wave at the injection port loses strength. This is expected, since the θ-β-M relation of supersonic flow dictates that the wave angle should decrease at higher Mach numbers for the same deflection, which is the constant polar angle of fuel injection in this context. The variable inclination and strength of the injection port shock wave allows it to reflect and interact differently with the examined nozzle geometry for each of the investigated air Mach numbers. For instance, while this shock wave undergoes few near-field reflections in case II-a (M = 2.4), a richer near-field shock environment is observed in case II-b (M = 2.7), and at M = 3.0, case II-c, this shock wave undergoes fewer near-field reflections but creates a flow that shocks severely at an axial location of about 0.04 m. It is again to be noted here that this behavior depends largely on the nozzle geometry examined, which means that each potential geometry or combustor design for a scramjet engine must be carefully examined on an individual basis, in order to carefully design and streamline the merits.

The comparison of helium mass fractions depicted in Figure 7c reveals that the recommendation of Yang et al. [6], which states that multiple shock waves should be utilized, whenever possible, applies very well to this current analysis. For better understanding of this statement, consider the ratio of the mixing length to the axial location of the terminating shock wave, both parameters being roughly estimated from Figures 7c and 7b, respectively. In the case of M = 2.4, this ratio is approximately equal to 55/35 = 1.57, while for M = 2.7, this ratio ≈ 70/50 = 1.40. Finally, for M = 3.0, 90/55 = 1.64. The significance of this ratio is that it describes how effective the shock/shear layer interaction is in creating local vortices within the shock train so that mixing almost completes inside the shock train. Based on this criterion, none of the three cases turns out to be perfect, since mixing continues to take place for a considerable distance downstream of the shock train. Nevertheless, the medium Mach number case (M = 2.7) is more "efficient," in the sense that it has the smallest ratio. Minimizing this ratio is a necessity for successful scramjet operation due to the extremely short residence times associated with scramjet flows. Recalling that case II-b has the richest shock train, this result provides favorable agreement with the results of Yang et al, which recommend that utilizing more shock waves is favorable for better mixing.

The question that poses itself is, for a given geometry, if the Mach number is increased or decreased, and the number of waves in the shock train reduces, does this mean that the train becomes ineffective? The answer is simply no. According to the θ-β-M relation, if the wave angle, β, which is a good representative of the wave strength, is held constant, the deflection angle, θ, has to increase or decrease, if the Mach number increases or decreases, respectively. This simple fact suggests that the polar angle of deflection can be allowed small increases or decreases to adapt for higher or lower Mach numbers, keeping the strengths of the injection-induced shock waves unchanged. No contradiction exists between this statement and the ones made earlier, which state that the injection angle should be kept small, because of two reasons. First, the maximum changes in the injection angle, dictated by the θ-β-M relation, are small, even for considerable changes in the flow Mach number, and second, these small changes adapt the injection of fuel to the energy level of the flow. A high Mach number flow, for instance, has an energy level high enough to still suppress the fuel to a thin boundary layer, even if the injection angle is slightly increased. A lower Mach number flow, on the other hand, is incapable of keeping a thin boundary layer, and thus, the injection angle has to be decreased to avoid excessive boundary layer growth and blockage.

Effect of Compressibility

To further strengthen the validity of the presented results, and to test the power of the used simulation code, some of the investigated supersonic cases were chosen for comparison against their subsonic counterparts. Figures 8a to 8c show cases I-a (parallel), I-b (5°), and I-e (normal) being compared side-by-side to three corresponding subsonic (M_{throat} = 0.35) cases of the same angles of injection. The helium flow rate was kept constant throughout the analysis of Figure 8, so as to facilitate a comparison based on the mass fractions. The effect of compressibility is clearly seen. While the fuel is incapable of penetrating the resistive supersonic airflow, even in the case of normal injection, penetration is achieved much more easily in the subsonic cases. Yet, a remarkable observation to be made from Figure 8 is that the supersonic and subsonic mixing lengths are comparable, in spite of the facts that (a) penetration is much more difficult in supersonic flows and (b) the fuel can only mix through the supersonic-to-subsonic shear layer. This observed behavior can only be attributed to the beneficial effects of shock/shear layer mixing enhancement in supersonic flows. The concentrated vorticity at the locations of interaction of the shock train with the air/fuel shear layer compensates for the negative effects of compressibility on mixing. Thus, to achieve good mixing in supersonic flows, the fuel does not need to "literally penetrate" the air flow, as some research on traverse fuel injection in supersonic flows suggests, because (a) the fuel never fully penetrates the airflow, even at normal injection, (b) the problems of flow blockage, larger total pressure losses, and boundary layer separation are major negative side effects of normal injection, and (c) scramjet flows always have shock trains that can be utilized for mixing enhancement through shock/shear layer interaction. Therefore, the results of this analysis on the effect of compressibility strengthen those of the two analyses presented on the effects of injection scheme and Mach number. Small injection angles are favorable for shock-wave-rich flows to promote mixing and increase the engine thrust.

IV. Conclusions

The simulations made in this work on the interaction of a gaseous fuel jet with a shock-wave-rich environment or airflow yielded the following conclusions. (a) Shock waves, usually inherent in scramjet flows, can be utilized positively for mixing enhancement. (b) Mixing of a fuel jet injected in supersonic airflow cannot not be fully accomplished through direct penetration of the airflow, but through an air/fuel shear layer. (c) If the shock train of the airflow can be utilized or altered to effectively interact with that shear layer, greater benefit can be made from the generated vorticity at the locations of shock/shear layer interaction. This added vorticity and the adverse pressure gradient across each shock wave aid in mixing the air and fuel streams across the shear layer and cause shear layer spreading, thus the vortices are allowed to grow in size downstream of each shock wave, which leads to better mixing. (d) Small oblique angles of injection are recommended for shock-wave-rich flows, as they provide better performance from the points of view of mixing, total pressure loss, flow blockage, and boundary layer separation. (e) The injection angle should be changed slightly according to the Mach number of the airflow, wherein the higher Mach numbers can tolerate larger angles, while the lower Mach numbers favor smaller angles to avoid excessive shocking.

Acknowledgments

This work was supported by the Space Vehicle Technology Institute under grant NCC3-989 jointly funded by NASA and DoD within the NASA Constellation University Institutes Project, with Claudia Meyer as the Project Manager. The DoD work was supported by the USAF and is gratefully acknowledged.

Technical support provided by Dr. Ryan Starkey is much appreciated.

The simulation code, CFDRC, was provided by ESI-Group. This support is gratefully acknowledged.

References

1. Ben-Yakar, A., "Experimental Investigation of Transverse Jets in Supersonic Cross-flows," Ph.D. Dissertation, Dept. of Mechanical Eng., Stanford Univ., Stanford, CA, Dec. 2000.

2. Huber, P. W., Schexnayder, C. J., and McClinton, C. R., "Criteria for Self-Ignition of Supersonic Hydrogen-Air Mixtures," NASA TP 1457, 1979.

3. Ben-Yakar, A., and Hanson, R. K., "Experimental Investigation of Flame-Holding Capability of a Transverse Hydrogen Jet in Supersonic Cross-Flow," Proc. Twenty-Seventh Symposium (Intl.) on Combustion, The Combustion Inst., Pittsburgh, PA, 1998, pp. 2173–2180.

4. Lee, S. H., "Characteristics of Dual Transverse Injection in Scramjet Combustor," Journal of Propulsion and Power, Vol. 22, No. 5, September–October 2006, pp. 1012 – 1019.

5. Huh, H., and Driscoll, J. F., "Measured Effects of Shock Waves on Supersonic Hydrogen-Air Flames," 32nd Joint Propulsion Conference and Exhibit, Lake Buena Vista, FL, July, 1996, AIAA-96-3035.

6. Yang, J., Kubota, T., and Zukoski, E. E., "Applications of Shock-Induced Mixing to Supersonic Combustion," AIAA Journal, Vol. 31, No. 5, May 1993, pp. 854-862.

7. Andreadis, D., "Scramjets integrate air and space," The Industrial Physicist, American Institute of Physics, August/September 2004 Issue, pp. 24 – 25.

8. Menon, S., "Shock-wave-induced mixing enhancement in scramjet combustors," AIAA 27th Aerospace Sciences Meeting, Reno, NV, Jan 1989, AIAA-89-0104.

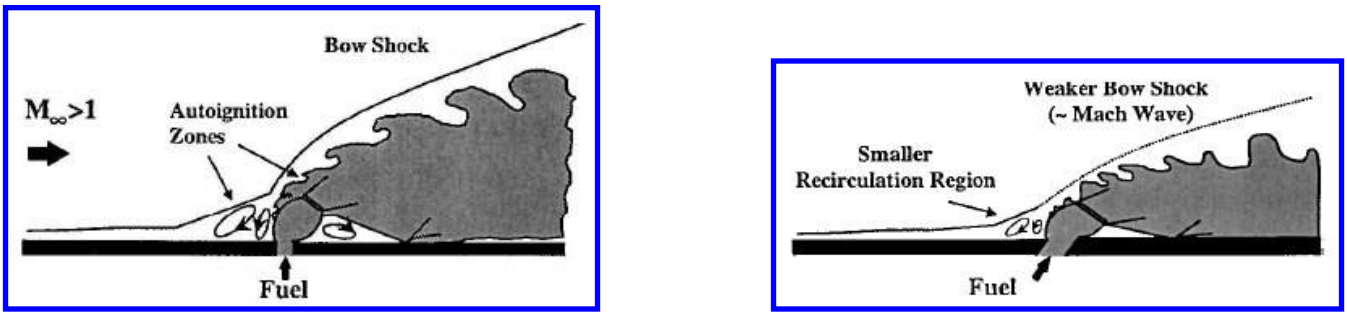

Figure 1. a) Traverse injection (left), and b) oblique injection (right) [1]

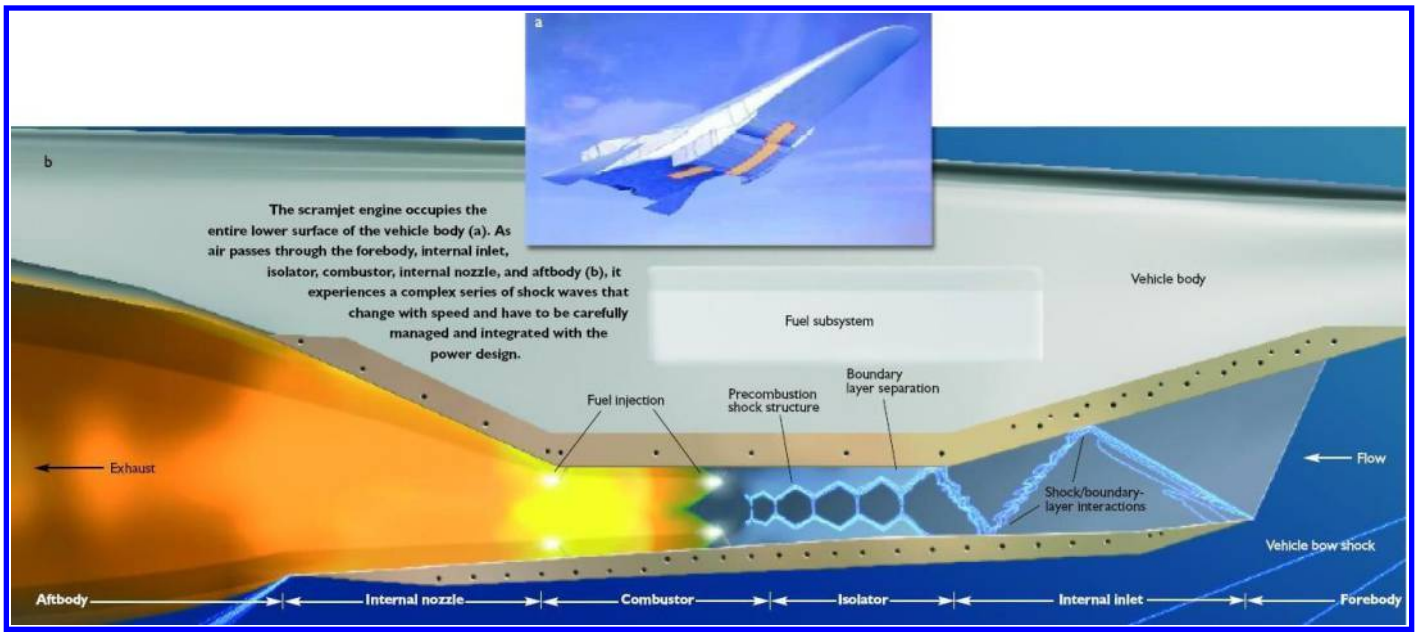

Figure 2. Shock-wave-rich nature of scramjet flows [7]

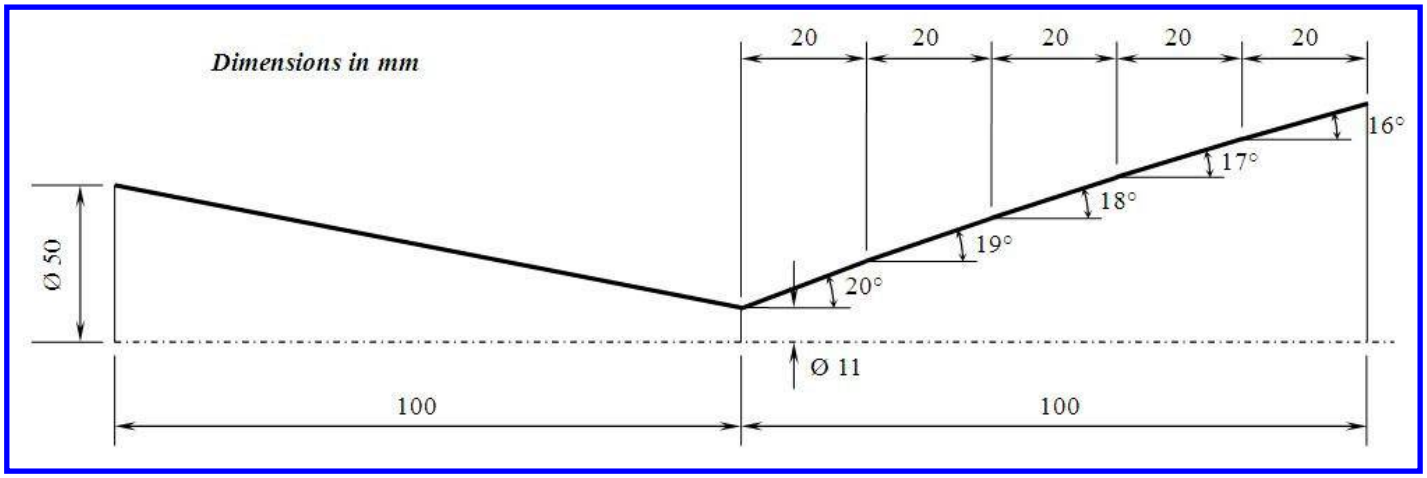

Figure 3a. Schematic of the implemented convergent-divergent nozzle geometry

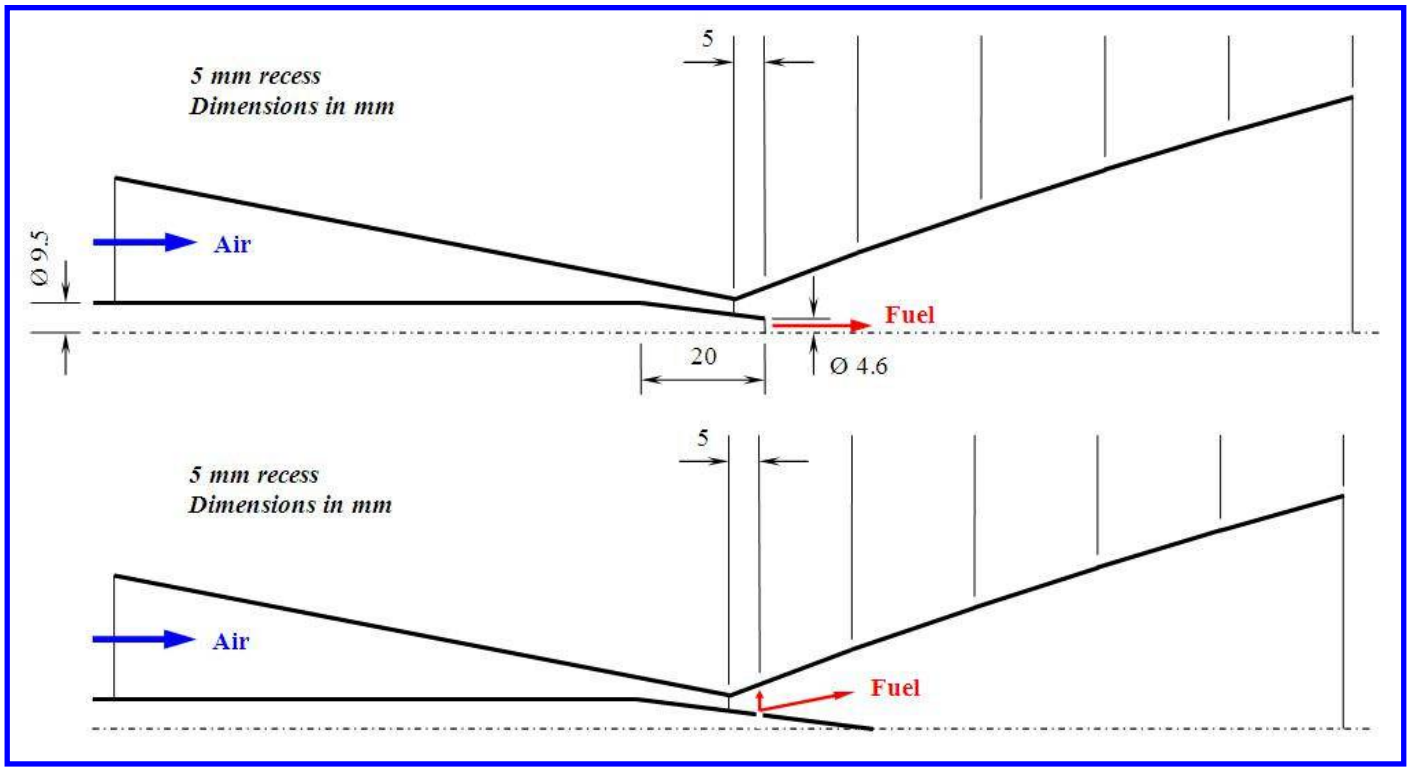

Figure 3b. Schematic of the fuel systems for parallel, oblique, and traverse injection

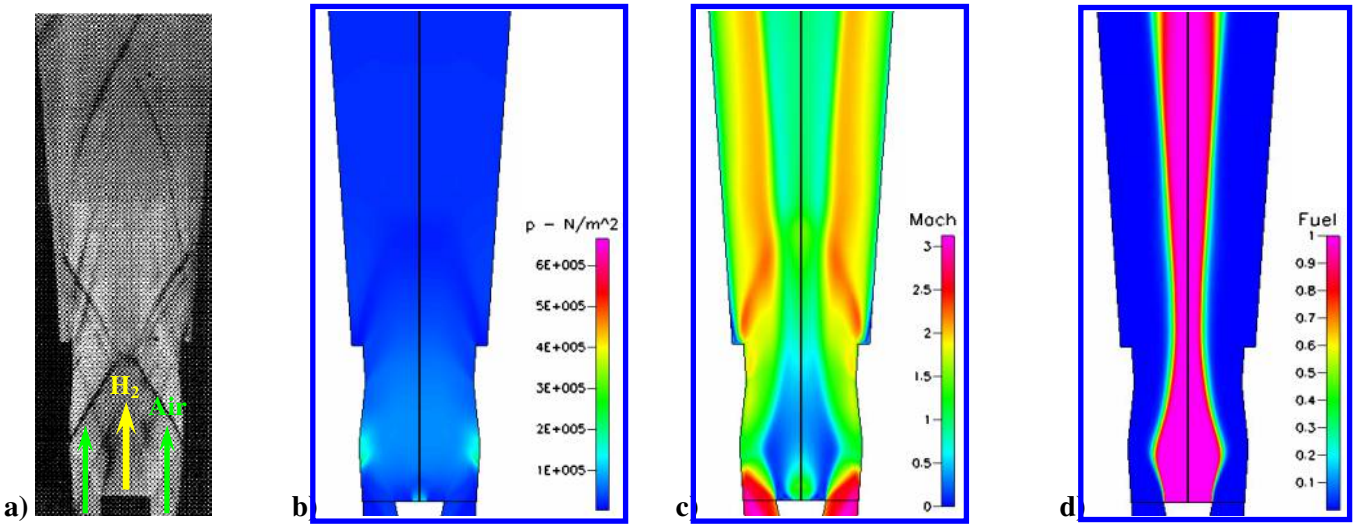

Figure 4. Code validation through the simulation of part of the experimental work done by Huh and Driscoll [5] on the effects of shock waves on supersonic hydrogen-air flames. Non-reacting conditions are considered. a) actual Schlieren image of the flow, b) static pressure, c) Mach number, and d) fuel mass fraction simulated profiles. Height of examined region = 25.4 cm; air Mach number at injection plane = 2.5; fuel Mach number = 1.0; fuel mass flow rate = 1 g/s; air stagnation pressure and temperature = 6.44 atm and 294 K, respectively; fuel static pressure = 1.12 atm.

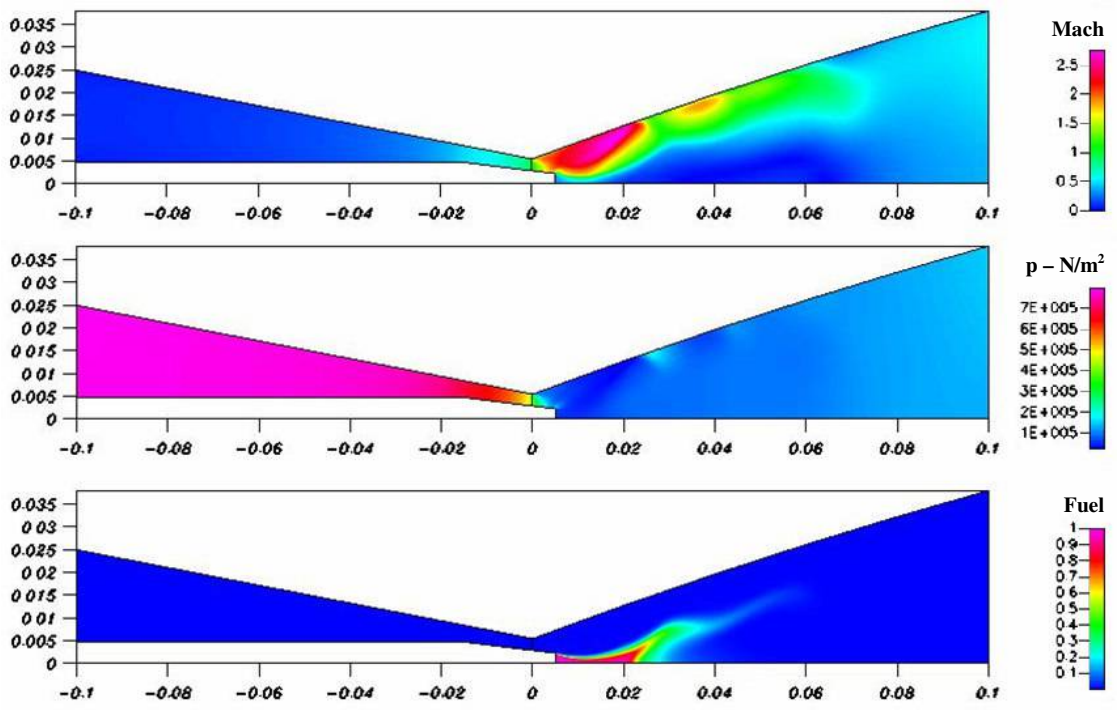

Figure 5a. Mach number, static pressure, and helium mass fraction profiles for case I-a (parallel injection, nominal maximum air Mach number = 2.7)

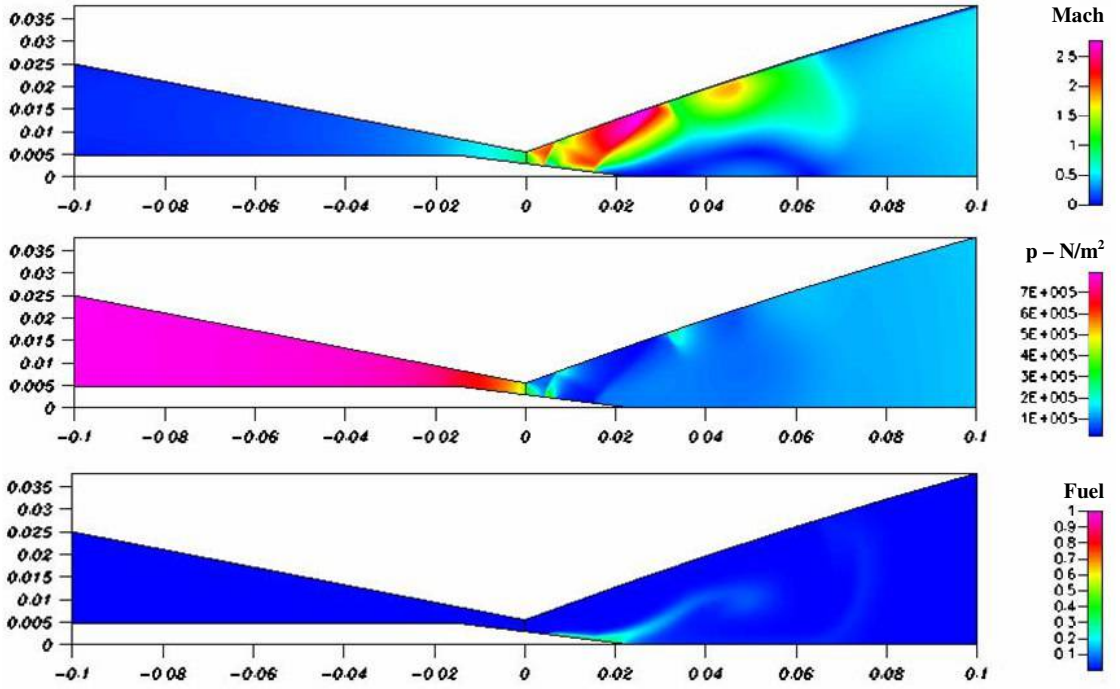

Figure 5b. Mach number, static pressure, and helium mass fraction profiles for case I-b (5° oblique injection, nominal maximum air Mach number = 2.7)

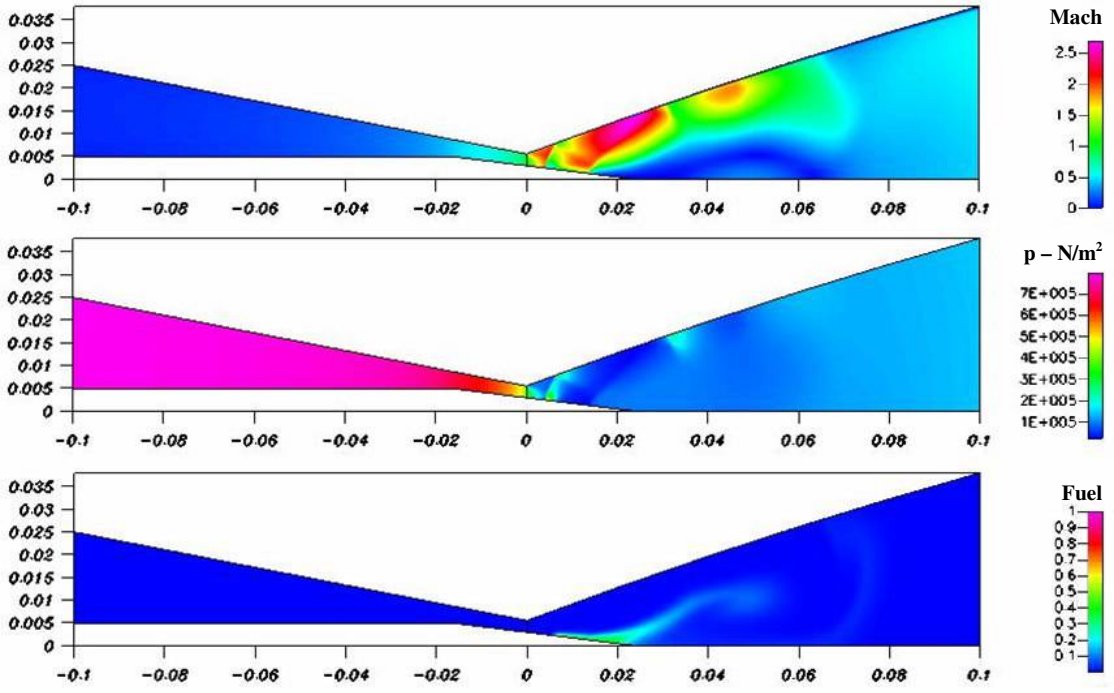

Figure 5c. Mach number, static pressure, and helium mass fraction profiles for case I-c (10° oblique injection, nominal maximum air Mach number = 2.7)

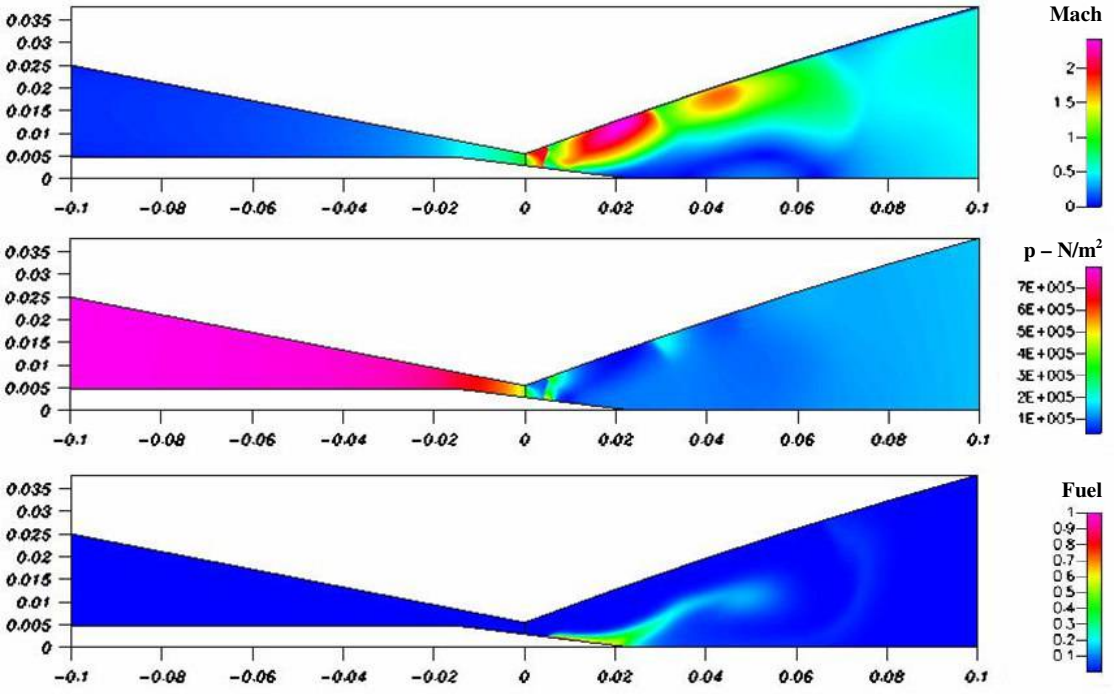

Figure 5d. Mach number, static pressure, and helium mass fraction profiles for case I-d (30° oblique injection, nominal maximum air Mach number = 2.7)

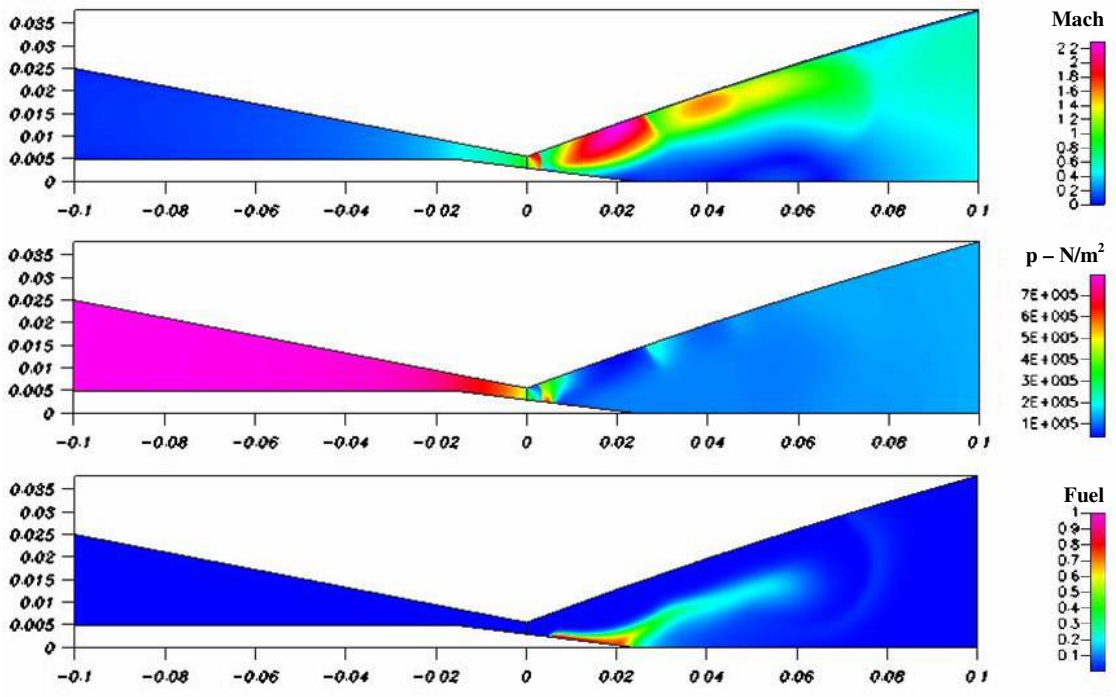

Figure 5e. Mach number, static pressure, and helium mass fraction profiles for case I-e (traverse injection, nominal maximum air Mach number = 2.7)

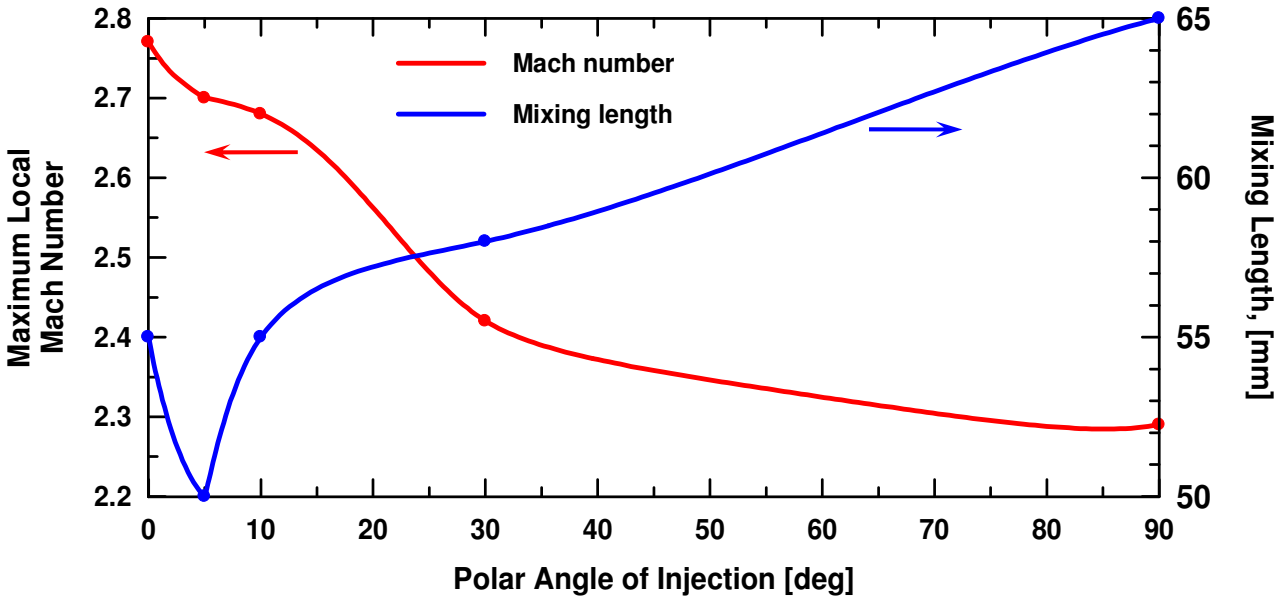

Figure 6. Variation of the maximum local Mach number and mixing length with the polar angle of injection

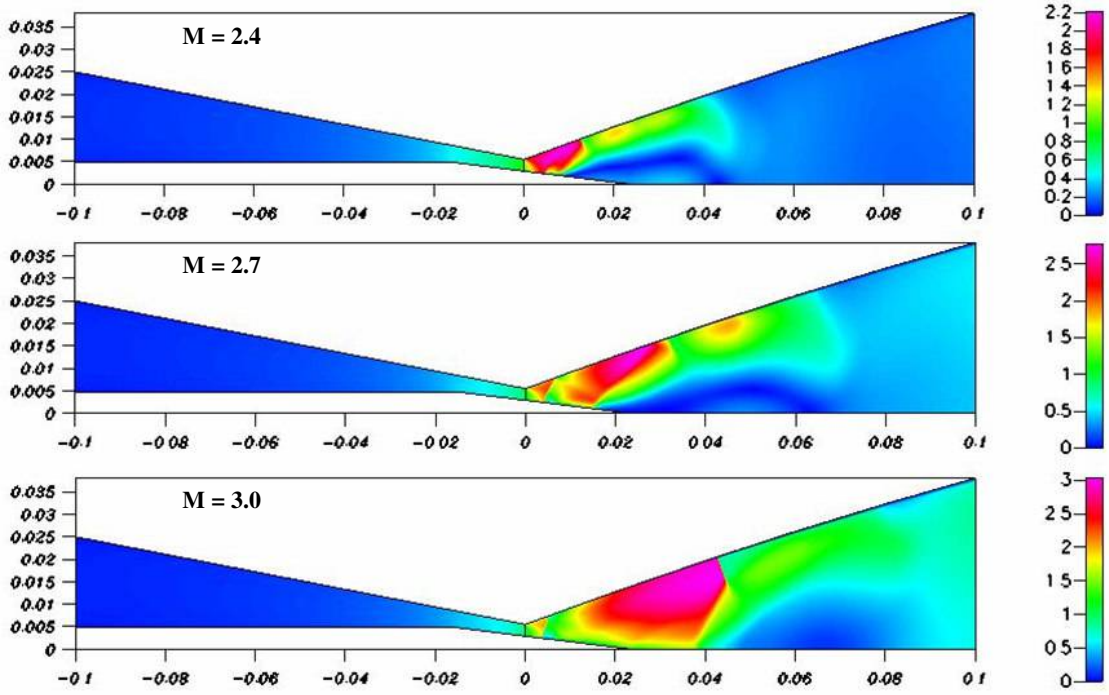

Figure 7a. Comparison of Mach number profiles for cases II-a (M = 2.4), II-b (M = 2.7), and II-c (M = 3.0), respectively (5° oblique injection)

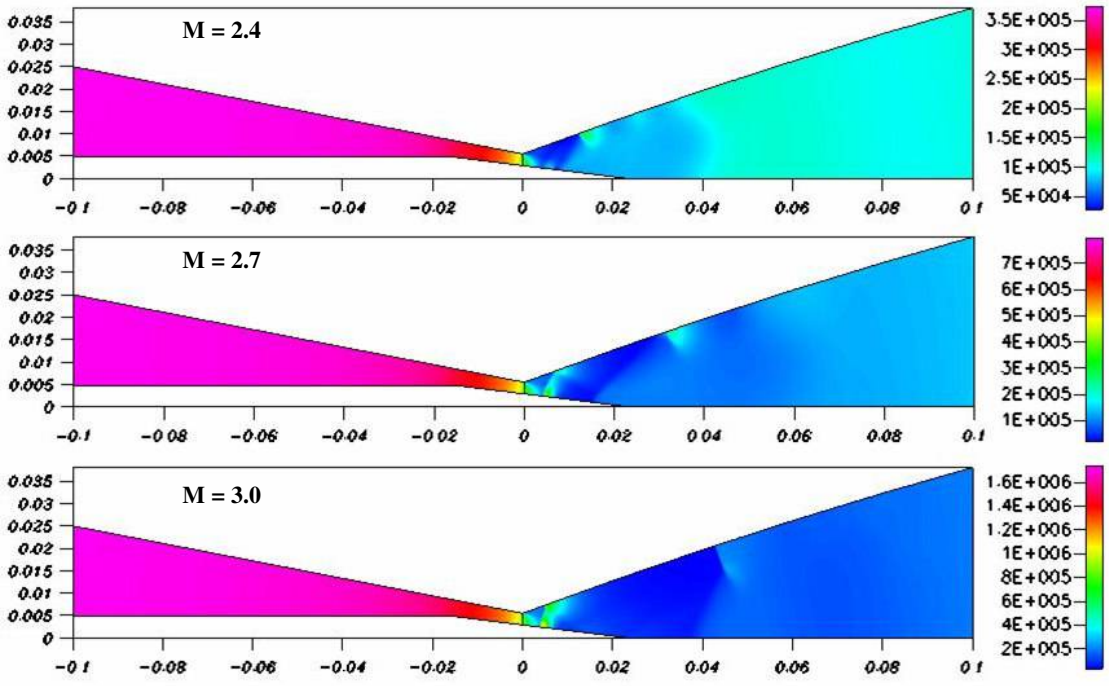

Figure 7b. Comparison of static pressure profiles [N/m^2] for cases II-a (M = 2.4), II-b (M = 2.7), and II-c (M = 3.0), respectively (5° oblique injection)

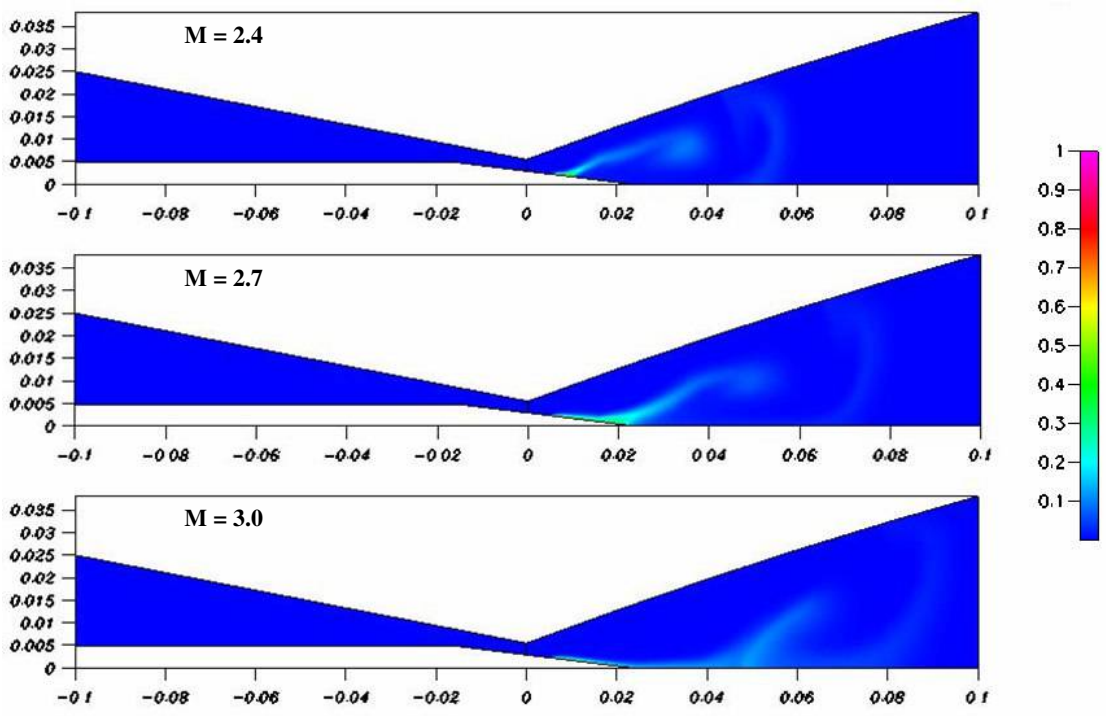

Figure 7c. Comparison of helium mass fraction profiles for cases II-a (M = 2.4), II-b (M = 2.7), and II-c (M = 3.0), respectively (5° oblique injection)

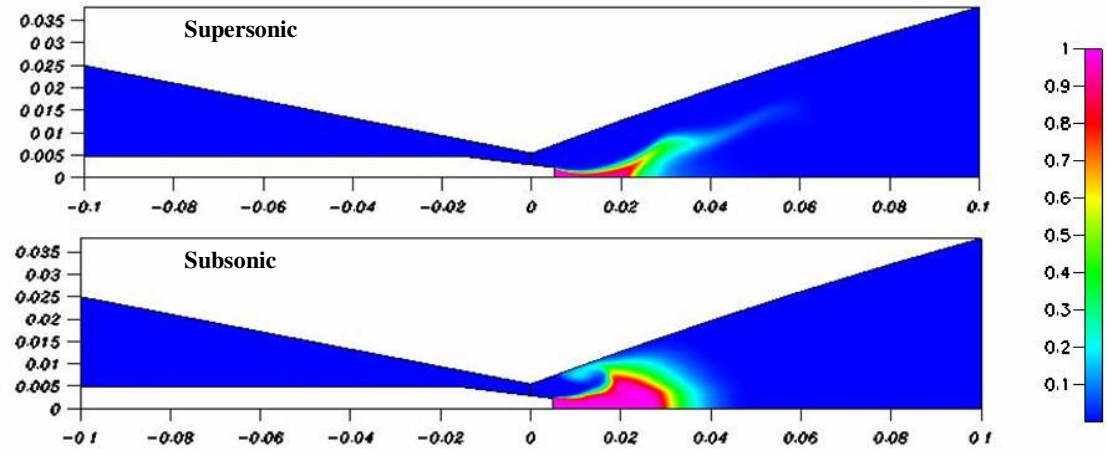

Figure 8a. Supersonic (Mach 2.7) vs. subsonic (M_{throat} = 0.35) behaviors for parallel injection

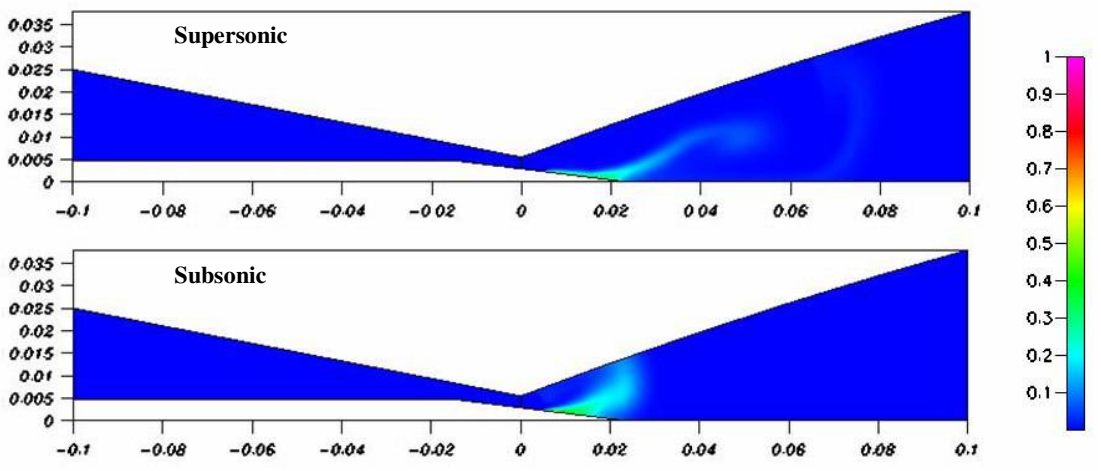

Figure 8b. Supersonic (Mach 2.7) vs. subsonic (M_{throat} = 0.35) behaviors for 5° oblique injection

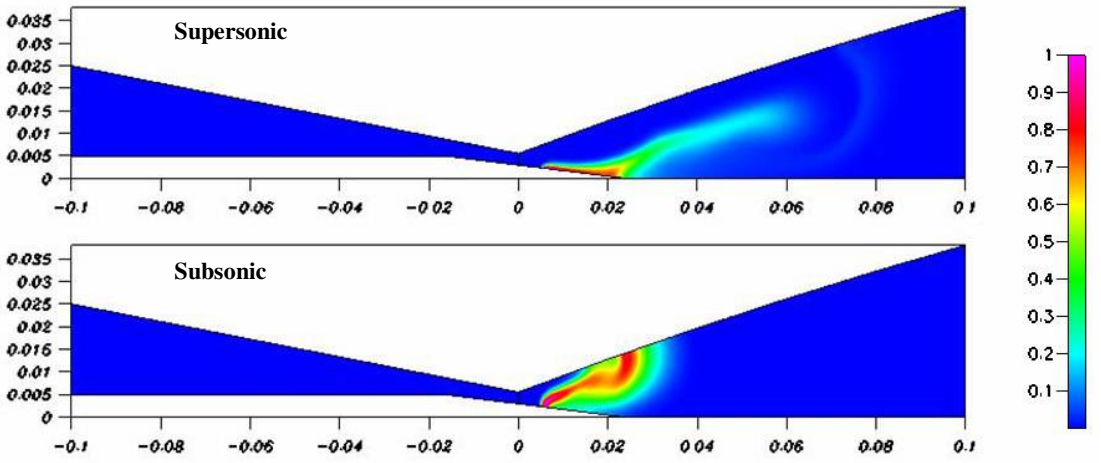

Figure 8c. Supersonic (Mach 2.7) vs. subsonic (M_{throat} = 0.35) behaviors for traverse injection